Correlations between neutral and charged pions produced in 300-GeV/c pp collisions

T. Kafka, F. LoPinto,* A. Brody,† R. Engelmann, J. Hanlon, and S. Sommars
State University of New York at Stony Brook, Stony Brook, New York 11794

W. A. Mann, F. T. Dao, J. Schneps, A. J. Segar, and H. Wald
Tufts University, Medford, Massachusetts 02155

R. Ammar, R. Davis, C. Eklund, L. Herder, N. Kwak, R. Riemer, R. Stump, and D. Zacrep
University of Kansas, Lawrence, Kansas 66045

K. Jaeger
Argonne National Laboratory, Argonne, Illinois 60439
(Received 23 March 1978; revised manuscript received 28 September 1978)

Neutral-pion production in pp interactions has been studied using 8000 photon conversions in the Fermilab 15-ft bubble chamber. Inclusive π^0 multiplicity moments and $\pi\pi$ correlation integrals are presented; f_2^{00} is determined to be $+3.0\pm0.8$. For the semi-inclusive π^0 multiplicity distributions we find $\langle n(\pi^0)\rangle_{n_-}$ to increase with n_-, while the dispersions are n_- independent. Results on f_2^{-0}, f_2^{00}, and f_{2,n_-}^{00} are compared to predictions of simple cluster models.

I. INTRODUCTION

Progress toward understanding high-energy multiparticle production has been hindered by a paucity of correlation measurements involving neutral pions. Previous experimental investigations of the neutral component of multipion production at Fermilab energies have been limited either by the low (~1.5%) photon-conversion efficiency of the bare 30-in. hydrogen bubble chamber, or by solid-angle restrictions in counter experiments.

We have used the Fermilab 15-ft Bubble Chamber, filled with liquid hydrogen and exposed to a beam of 300-GeV/c protons, to study inclusive and semi-inclusive production of photons from π^0 decays. We report the first results obtained at Fermilab energies on π^0 multiplicity moments and correlation integrals involving two or more neutral pions, as well as new measurements of the inclusive π^0 cross section and the average inclusive and semi-inclusive π^0 multiplicities. Wherever possible, our values are compared to published data from experiments performed both at Fermilab and at lower energies.[1-7]

II. EXPERIMENTAL PROCEDURE

A. Film exposure

Primary proton-proton interactions, photon conversions, and neutral-particle decays were recorded in 23 000 triad photographs obtained with the Fermilab 15-ft Bubble Chamber exposed to a beam of 300-GeV/c protons. An average of 1.4 protons per picture were incident upon the scanning fiducial volume; 11 500 primary pp interactions and 19 000 vees (photon conversions and neutral-particle decays) were found. The entire film was scanned twice, with the resulting scanning efficiency of 0.99 ± 0.01 for the primary interactions and $\epsilon = 0.97\pm0.01$ for the vees.

All vees recorded in a frame containing one or more primary interactions were measured on Vanguard film-plane digitizers with projected images about half life-size and were processed using the geometric-reconstruction program TVGP and the kinematic-fitting program SQUAW. For each vee, fits to the following hypotheses were attempted:

$$\gamma + p_{\text{spectator}} \to e^+ + e^- + p_{\text{spectator}},$$

$$\gamma + e_{\text{spectator}} \to e^+ + e^- + e_{\text{spectator}},$$

$$K^0 \to \pi^+ + \pi^-,$$

$$\Lambda^0 \to p + \pi^-,$$

and

$$\bar{\Lambda}^0 \to \pi^+ + \bar{p}.$$

After four measuring passes 63.5% of the vees yielded 3-constraint (3C) fits to production vertices, 27% gave 1C fits only, and 9.5% yielded no fits, or were unmeasurable. An event which yielded a 3C fit was retained for analysis, if its primary vertex occurred within a rectangular volume extending 280 cm along the beam direction, and its conversion/decay vertex occurred both within a spherical volume of 326-cm diameter and between two horizontal planes located 100 cm above and below the beam plane (secondary fid-

ucial volume). In this way a minimum 32 cm of measurable track length is ensured for the vee conversion/decay tracks. Out of 8380 3C γ fits which had both their production and conversion vertices within the appropriate fiducial volume, 1250 were ambiguous with 3C K^0 or $\Lambda^0/\overline{\Lambda}^0$ hypotheses. About 75% of these ambiguous fits were found to have $|\vec{p}(e^-)\times\vec{p}(\gamma)|$ less than 0.02 GeV/c and were included in our final sample.

B. γ losses and weights

Properties of the γ's which yielded kinematic fits were carefully examined to identify all significant losses of photons in the experiment. For each loss, a compensating weight was included in the cross-section calculation:[8,9]

1. Losses in scanning. These were corrected for by weight $w_1 = 1/\epsilon$.

2. γ track length. Photons which did not convert within the secondary fiducial volume escaped undetected, and those having their track lengths shorter than 60 cm were detected with reduced efficiency since they could be obscured by the tracks of charged secondary particles. The latter effect was found to be more severe for events with higher charged-particle multiplicity n_c (see Fig. 1). For events with $n_c \leq 12$ ($n_c \geq 14$) γ's were removed from the data sample if their track lengths were less than a minimum length $l_{\min}$ of 10 cm (30 cm). All remaining γ's were assigned a weight w_2 based on their potential paths[10] within the fiducial volume and their momentum-dependent conversion lengths $\lambda(p)$[11]:

$$w_2 = \{\exp[-l_{\min}/\lambda(p)] - \exp[-l_{\text{pot}}/\lambda(p)]\}^{-1} .$$

An additional depletion of photons in the track length interval $l_{\min} < l < 60$ cm was accounted for by applying an l-dependent weight w_2' to bring the weighted photon numbers into agreement with the expected distribution (dashed line in Fig. 1, Ref. 12) normalized to the data for $l > 60$ cm.[13]

3. Low-momentum $e^\pm$ tracks. Since reliable measurement of electron tracks was only possible for $p_{\text{lab}}(e^\pm) > E_0 = 25$ MeV, losses were incurred in both low-momentum γ's and in energetic γ's having highly unequal energy-sharing between their conversion electrons.

Correction for the unobserved asymmetric γ's was accomplished by weighting the observed γ's according to the shape of the distribution in the energy-sharing ratio,

$$R = E_{\text{lab}}(e^+)/[E_{\text{lab}}(e^+) + E_{\text{lab}}(e^-)] .$$

For any given value of the photon momentum, the values of R not accessible to our experiment are $R < R_0$ and $R_0 > (1 - R_0)$, where $R_0 = E_0/p_{\text{lab}}(\gamma)$. The undetected fraction of the R distribution is thus appreciable only for low-momentum γ's. In Fig. 2 we compare our data for $p_{\text{lab}}(\gamma) < 0.5$ GeV/c with the predictions of a QED calculation[14] folded with the observed distribution in $p_{\text{lab}}(\gamma)$. A depletion is observed in Fig. 2(a) for R close to 0 and 1

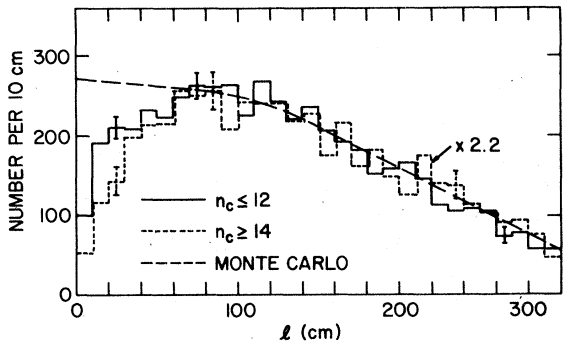

FIG. 1. Distribution in the γ track length for events with charged-particle multiplicity $n_c \leq 12$ (solid line) and $n_c \geq 14$ (dotted line, data multiplied by a factor of 2.2). The dashed line represents the expected distribution (see Ref. 12). (All curves are normalized to $l > 60$ cm.)

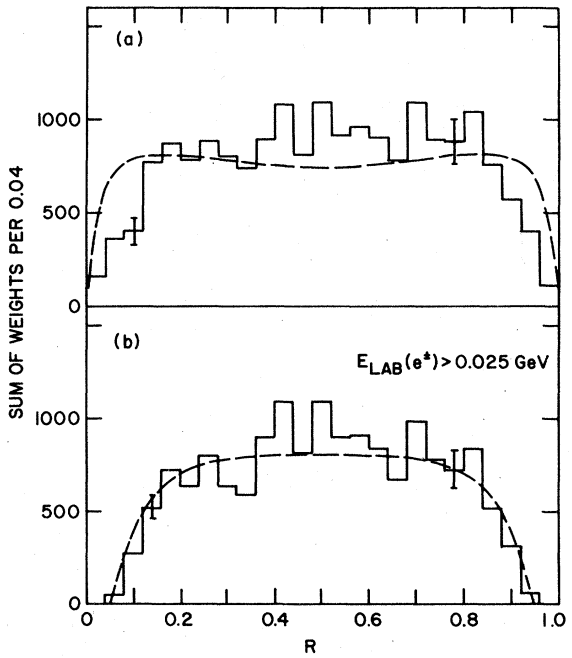

FIG. 2. Distribution in the energy-sharing ratio R (solid line) for $p_{\text{lab}}(\gamma) < 0.5$ GeV/c: (a) no cut on $E_{\text{lab}}(e^\pm)$, and (b) $E_{\text{lab}}(e^\pm) > 0.025$ GeV. The dashed lines represent a QED calculation (see Ref. 14) folded with the observed distribution in $p_{\text{lab}}(\gamma)$.

while a removal of γ's with $E_{1ab}(e^{\pm}) < E_0$ results in an agreement between the measured and expected distributions as illustrated in Fig. 2(b). Thus, a weight w_3 has been assigned to each γ having both $p_{1ab}(\gamma) > p_0 = 2E_0$ and $E_{1ab}(e^{\pm}) > E_0$ according to

$$w_3 = \left(\int_{R_0}^{1-R_0} \frac{d\sigma}{dR}\, dR \Big/ \int_0^1 \frac{d\sigma}{dR}\, dR \right)^{-1}.$$

In calculating w_3 we used the QED formulas of Ref. 14 which include photon conversions in the electric fields of both the nucleus and orbital electron of atomic hydrogen.

We corrected for losses of γ's having both conversion electrons slow, $E_{1ab}(e^{\pm}) < E_0$, by weighting γ's in the backward center-of-mass (c.m.) hemisphere according to the number of γ's observed in the symmetric region of the forward hemisphere (weight w_3').

4. γ production at small angles. The $\cos\theta_{c.m.}$ distribution for photons having $p_{1ab}(\gamma) > p_0$ and $p_{\text{beam rest frame}}(\gamma) > p_0$ is shown in Fig. 3. A depletion is observed for $\cos\theta_{c.m.} > 0.8$, corresponding to $\theta_{1ab} < 2°$. We ascribe this loss to the fact that most of the charged secondary tracks in a high-energy hadron collision are highly collimated and often cover a conversion/decay of a fast particle moving at a small θ_{1ab}. Since this loss was not completely accounted for by weights w_1 and w_2,[13] we applied a correction w_4 to our data in the forward c.m. hemisphere to restore the c.m. symmetry.

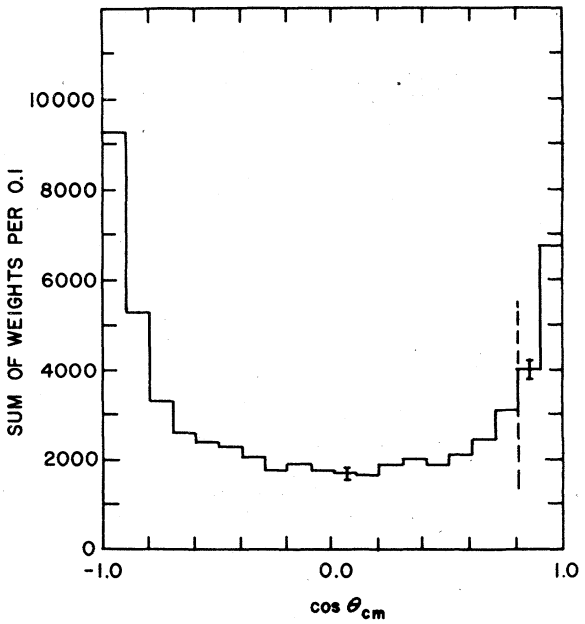

FIG. 3. Distribution in the $\cos\theta_{c.m.}(\gamma)$ for $p_{1ab}(\gamma) > p_0$ and $p_{\text{beam rest frame}}(\gamma) > p_0$.

5. Vertex ambiguities.

(a) *Ambiguity in primary vertex assignment.* In 4% of all γ's 3C fits to two different primary vertices were obtained. In such cases both 3C fits were retained and each was assigned a weight according to its relative χ^2-probability p, $p_i/(p_1+p_2)$, $i = 1, 2$.

(b) γ's *from secondary vertices.* In a sample of 240 frames, all γ conversions and all visible hadronic vertices were digitized. Kinematic fits to all vertices were tried for each γ. From these measurements it was determined that the fraction of γ's which yielded a 3C fit to a primary pp vertex in our experiment, but which were actually produced at a secondary vertex, was (0.06 ± 0.02).

6. Compton scattering: Each γ in our data received a weight w_6 which was the inverse probability for a photon to escape large-angle Compton scattering in the bubble chamber. The values for w_6 varied from 1.04 for $p_{1ab}(\gamma) < 100$ MeV/c to 1.0 for $p_{1ab}(\gamma) > 1.0$ GeV/c.

Every γ which yielded a 3C fit in our experiment was assigned a total weight determined by the above procedures:

$$w = w_1 w_2 w_2' w_3 w_4 w_4' w_5 w_6 .$$

The average value of w was 9.7 ± 0.4. The contributions from individual factors are summarized in Table I.

At this stage in the experiment there remained a sample of vees which were regarded to be unmeasurable. A special edit of these vees was performed in order to evaluate which ones were likely to be within the fiducial volume, to be actually pointing to a primary pp interaction, and to be unaccounted for by one of the weights. A total of 505 unmeasurable vees were accepted by the edit for subsequent analysis and each was assigned an average total weight.

C. The multiplicity distribution and cross-section calculation

From our scanning data we determined the charged-particle multiplicity distribution. Standard corrections were applied for miscounting the number of charged prongs from production vertices due to close-in vees, due to secondary interactions of charged and neutral particles, and due to π^0 Dalitz decays.[8] Our corrected distribution for $n_c \geq 4$ is found to be in agreement with published results from a study of pp collisions in the Fermilab 30-in. Bubble Chamber at the same energy.[15]

We did not measure the numbers of two-prong elastic and inelastic events, but rather inferred them using published values for the ratios $\sigma_{2\ el}$/

TABLE I. Summary of γ weights.

Weight		Value [a]
Scanning efficiency	w_1	1.03 ±0.01
Potential length	w_2	8.4 ±1.0
Track length	w_2'	1.03 ±0.01
Energy sharing	w_3	1.09 ±0.01
Low energy	w_3'	1.005±0.003
cos $\theta_{c.m.}$	w_4	1.07 ±0.01
γ's from secondary interactions	w_5	0.94 ±0.02
Compton scattering	w_6	1.002
Total		9.7 ±0.4

[a]Averaged over all 3C γ fits.

$\sigma_{n_c\geq 4}$ and $\sigma_{2\ \mathrm{inel}}/\sigma_{n_c\geq 4}$.[15] In this way, the number of inelastic pp collisions in our data was determined to be 9185 ± 136. The total number of pp collisions was determined to be 11 446 events, corresponding to 3.42 μb/event. After a correction for the 4% meson contamination in our proton beam, we obtained $\sigma_{\mathrm{tot}}(pp) = 39.21 \pm 0.92$ mb, which compares favorably with the value of 39.47 ± 0.16 mb extrapolated from high-precision measurements at incident momenta up to 280 GeV/c.[16]

III. RESULTS

A. γ and π^0 cross sections

We have measured the cross section for inclusive photon production to be $\sigma(\gamma) = 269.8 \pm 11.5$ mb,[17] from which we obtained for the inclusive π^0 production cross section a value of $\sigma_\gamma(\pi^0) = 134.9 \pm 5.8$ mb. In addition, we measured $\sigma(\pi^0)$ directly from the π^0 signal observed in the $\gamma\gamma$ invariant-mass distribution shown in Fig. 4, and obtained $\sigma_{\gamma\gamma}(\pi^0) = 110 \pm 20$ mb. Although our values for $\sigma_\gamma(\pi^0)$ and $\sigma_{\gamma\gamma}(\pi^0)$ are consistent, the fact that $\sigma_{\gamma\gamma}(\pi^0)$ is lower suggests that some photons may originate from processes other than π^0 decay. A possibly significant source of photons is the η meson if produced copiously. From the small enhancement in the η region of our $\gamma\gamma$ invariant mass distribution (see Fig. 4) we estimate $\sigma(\eta)B(\eta \to \gamma\gamma)$ to be 9 ± 6 mb, yielding the upper limit $\sigma(\eta) < 45$ mb at the 90% confidence level. Thus the overall inclusive η/π^0 ratio in 300-GeV/c pp collisions is less than 0.37, to be compared to the value of 0.45 ± 0.03 observed for transverse momenta greater than 2 GeV/c.[18] Since the η enhancement in our data is not statistically significant, we assume in the following analysis that all photons originate from π^0 decays.

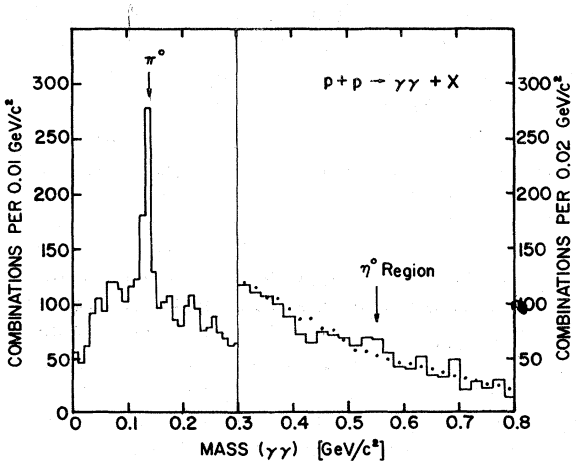

FIG. 4. Invariant-mass distribution for $\gamma\gamma$ pairs. The dotted line represents a background obtained by combining photons from different events and normalized to $m(\gamma\gamma) > 0.6$ GeV/c^2.

B. Inclusive π^0 moments

We have obtained the average photon multiplicity $\langle n_\gamma \rangle = \sum w_i / N_{\mathrm{inel}} = 8.58 \pm 0.37$. From 2276 events in our data sample which contain two or more observed γ's, the average number of photon pairs was determined to be

$$\tfrac{1}{2}\langle n_\gamma (n_\gamma - 1)\rangle = \tfrac{1}{2} \sum_i \sum_{j \atop i \neq j} w_i w_j / N_{\mathrm{inel}} = 47.07 \pm 4.11 .$$

The values of the first three binomial moments of the π^0 multiplicity distribution have been calculated from the corresponding moments of the γ multiplicity distribution. Definitions and measured values of the resulting π^0 multiplicity moments and correlations integrals are summarized in Table II. Using the values of $f_2^{--} = 1.21 \pm 0.12$ and $f_2^{+-} = 4.37 \pm 0.10$ obtained from our charged-particle multiplicity distribution, we note that the

TABLE II. π^0 multiplicity moments and correlation integrals.

Quantity	Definition	Value
$\langle n_0 \rangle$	$\frac{1}{2}\langle n_\gamma \rangle$	4.3± 0.2
$\langle n_0(n_0-1) \rangle$	$\frac{1}{4}\langle n_\gamma(n_\gamma-1) \rangle - \frac{1}{4}\langle n_\gamma \rangle$	21.4± 2.0
$\langle n_0(n_0-1)(n_0-2) \rangle$	$\frac{1}{8}\langle n_\gamma(n_\gamma-1)(n_\gamma-2) \rangle - \frac{3}{8}\langle n_\gamma(n_\gamma-1) \rangle + \frac{3}{8}\langle n_\gamma \rangle$	127 ±21
D_0	$(\langle n_0(n_0-1) \rangle + \langle n_0 \rangle - \langle n_0 \rangle^2)^{1/2}$	2.7± 0.2
f_2^{00}	$\langle n_0(n_0-1) \rangle - \langle n_0 \rangle^2$	3.0± 0.8
f_3^{000}	$\langle n_0(n_0-1)(n_0-2) \rangle - 3\langle n_0(n_0-1) \rangle \langle n_0 \rangle + 2\langle n_0 \rangle^3$	9 ± 8
$\langle n_- n_0 \rangle$	$\sum_{n_-} n_- \langle n_0 \rangle_{n_-} N_{n_-}/N_{\text{inel}}$	15.9± 0.4
f_2^{-0}	$\langle n_- n_0 \rangle - \langle n_- \rangle \langle n_0 \rangle$	2.3± 0.7

correlation integrals satisfy the inequalities $f_2^{+-} > f_2^{00} > f_2^{-0} > f_2^{--}$, in agreement with a previous observation that correlations are stronger for neutral pairs than for pairs with net charge.[19]

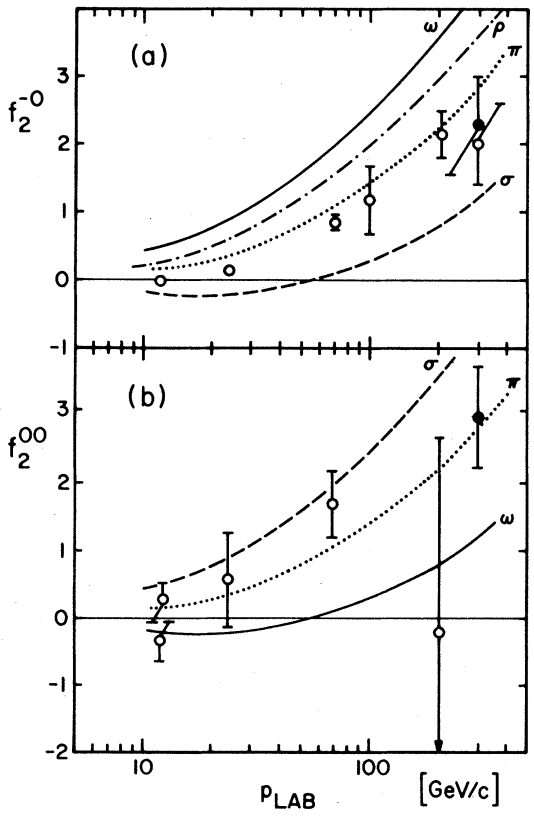

FIG. 5. The correlation integrals (a) f_2^{-0}, and (b) f_2^{00} from pp reactions as a function of beam momentum. Data are from Refs. 1 through 7 (open circles) and this experiment (full circle). The curves represent model calculations from Ref. 20.

The dependence of f_2^{00} and f_2^{-0} on incident proton momentum as determined by our data and other experiments (see Refs. 1–7) is shown in Fig. 5. The values of both correlation integrals are found to increase with increasing beam momentum in a similar way.

We compare the experimental values of f_2^{00} and f_2^{-0} with predictions of several simple cluster models.[20] In these models, "clusters" of definite isospin are created in a collision, and subsequently decay into the observed secondary pions.[21] Clusters in the σ model have isospin $I=0$ ($\pi^+\pi^-$, $\pi^0\pi^0$), while clusters in the ρ model have $I=1$ ($\pi^+\pi^0$, $\pi^-\pi^0$, $\pi^+\pi^-$). It can be seen in Fig. 5 that the predictions of the σ, ρ, and ω models increase with energy in a way similar to the data, but only a mixture of several cluster types could reproduce the observed numerical values. The dotted curve shows that a model incorporating independent emission of single pions can also reproduce the data.[20,22]

C. Semi-inclusive π^0 moments

The average π^0 multiplicity for a fixed number of negative secondary particles, $\langle n_0 \rangle_{n_-}$, is given in Fig. 6. A linear increase with charged-particle multiplicity is observed through $n_- = 8$, followed by a decrease reflecting limits imposed by phase space. From a fit using the form $\langle n_0 \rangle_{n_-} = a + bn_-$ for $n_- \leq 8$ we obtain $a = 2.25 \pm 0.15$ and $b = 0.64 \pm 0.04$. It has been suggested that the slope b is not zero due to a mixing of diffractive and nondiffractive samples, each having $b = 0$.[23] When we limit the fit to n_- between 3 and 8 to include only multiplicities with a negligible fraction of diffractive events,[24] we obtain for b a value of 0.59 ± 0.09 which is still significantly different from zero.

As shown in Fig. 6, the dependence of the second moment $\langle n_0(n_0-1) \rangle_{n_-}$ on n_- is qualitatively similar

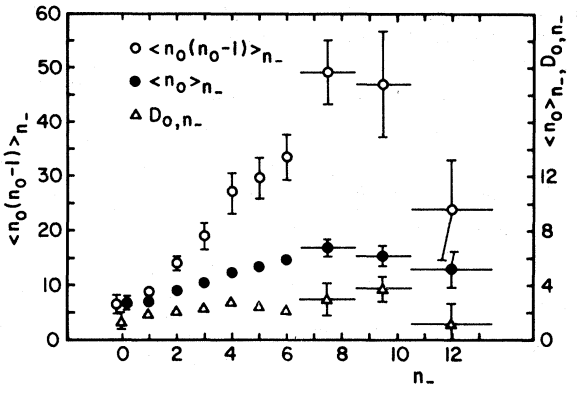

FIG. 6. Semi-inclusive moments of the π^0 multiplicity distribution: the average number of neutral pions $\langle n_0 \rangle_{n_-}$ (full circles), the number of π^0 pairs $\langle n_0(n_0-1) \rangle_{n_-}$ (open circles), and the dispersion D_{0,n_-} (triangles), plotted versus the number of produced negative particles.

to that of $\langle n_0 \rangle_{n_-}$. For $n_- \leq 8$, we may approximate $\langle n_0(n_0-1) \rangle_{n_-} = c + dn_-$ with $c = 4.2 \pm 1.0$ and $d = 5.3 \pm 0.4$. Figure 6 also indicates that dispersions D_{0,n_-} of the semi-inclusive π^0 multiplicity distributions do not vary significantly with n_-.

Our results for the semi-inclusive correlation integral f^{00}_{2,n_-} are given in Fig. 7 for $n_- \leq 6$. For comparison we have included in Fig. 7(a) the only other measurements of f^{00}_{2,n_-}, one at 12.4 GeV/c (Ref. 1) and another at 69 GeV/c (Ref. 3). The data at 12.4 GeV/c are severely limited by phase space. The data at 69 GeV/c and our 300-GeV/c results display similar trends. We compare our data on f^{00}_{2,n_-} with model predictions in Fig. 7(b). Agreement is obtained with the expectation of the independent-single-pion-emission model,[20,22] while the curves for the ω and σ clusters do not overlap the data.

Comparison of our results for f^{-0}_2, f^{00}_2, f^{00}_{2,n_-} with theoretical predictions shows that multipion production is not dominated by emission of a single type of cluster (σ, ρ, or ω). Our data can be accommodated by phenomenology which does not invoke cluster production (π model,[20] critical-fluid model[22]). There is, however, ample evidence that the observed correlations among charged particles cannot be explained by independent emission of single pions.[25] It thus remains for future models of multiparticle production to incorporate the production of neutral particles in a realistic way.

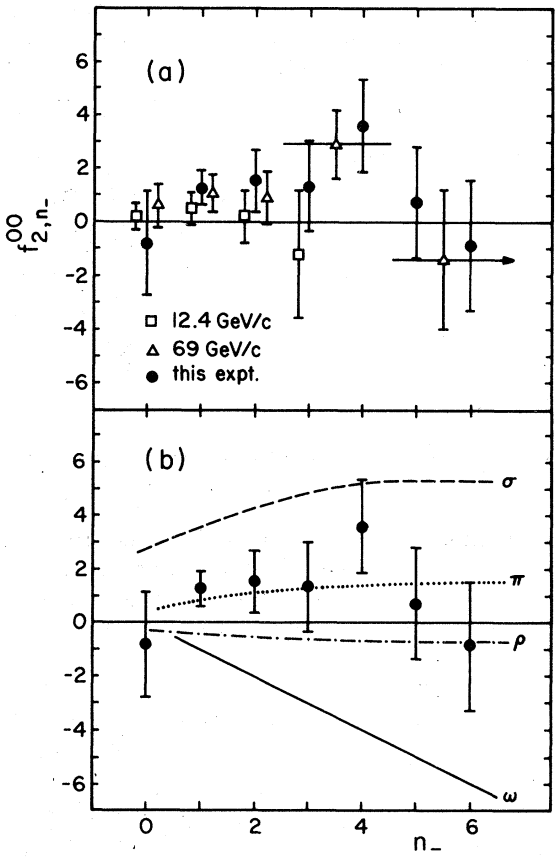

FIG. 7. (a) The semi-inclusive π^0 correlation integral f^{00}_{2,n_-} at 12.4 GeV/c (squares) (Ref. 1), at 69 GeV/c (triangles) (Ref. 3), and at 300 GeV/c (this experiment, full circles). (b) The semi-inclusive correlation integral f^{00}_{2,n_-} at 300 GeV/c (this experiment). The curves represent model calculations from Ref. 20.

ACKNOWLEDGMENTS

We thank the staff of the Neutrino Laboratory of the Fermi National Accelerator Laboratory for their assistance during the experimental runs. We are indebted to the scanning and measuring personnel at Kansas, Stony Brook, and Tufts Universities for their diligent work. We also wish to acknowledge helpful discussions with J. Kubar-Andre and G. Thomas. This work was supported in part by the National Science Foundation (at the University of Kansas and the State University of New York at Stony Brook) and in part by the U. S. Department of Energy (at the Argonne National Laboratory and Tufts University).

*Present address: Argonne National Laboratory, Argonne, Illinois 60439.
†Present address: Syracuse University, Syracuse, N. Y. 13210.

[1]12.4 GeV/c: J. H. Campbell *et al.*, Phys. Rev. D 11, 3824 (1973); D. Swanson *et al.*, Phys. Lett. 48B, 479 (1974); K. Jaeger *et al.*, Phys. Rev. D 11, 1756 (1975).
[2]12 and 24 GeV/c: K. von Holt *et al.*, Nucl. Phys. B103, 221 (1976).
[3]69 GeV/c: M. Boratav *et al.*, Nucl. Phys. B111, 529 (1976).
[4]102 GeV/c: J. W. Chapman *et al.*, Phys. Lett. 47B, 465 (1973).
[5]100 GeV/c: M. Alston-Garnjost *et al.*, Phys. Rev. Lett. 35, 142 (1975).
[6]205 GeV/c: K. Jaeger *et al.*, Phys. Rev. D 11, 2405 (1975).
[7]300 GeV/c: A. Sheng *et al.*, Phys. Rev. D 11, 1733 (1975).
[8]F. J. LoPinto, Ph.D. thesis, State University of New York, Stony Brook, N.Y., 1978 (unpublished).
[9]A more detailed account of the weight determination in our experiment can be found in Ref. 8. Similar methods used in the investigations of photon production in other bubble-chamber experiments are described in detail e.g. in Refs. 1 and 6.
[10]$l_{\rm pot}$ is the distance between the conversion vertex and the edge of the secondary fiducial volume, measured along the γ direction of flight.
[11]T. M. Knasel, DESY Reports Nos. 70/2 and 70/3 (unpublished).
[12]The dashed curve in Fig. 1 is a result of a Monte Carlo calculation incorporating the actual γ momentum distribution and the distribution in position of the primary pp collision vertices in the bubble chamber. The momentum dependence of the photon conversion and the limitation imposed by the fiducial volumes were taken into account.
[13]Inclusive γ production cross section was also calculated using a minimum length cut of 60 cm and $w_2'=1$. Results were the same as those obtained using the procedure of Sec. II B.
[14]Y. Tsai, Rev. Mod. Phys. 46, 815 (1974).
[15]A. Firestone *et al.*, Phys. Rev. D 10, 2080 (1974).
[16]A. S. Carroll *et al.*, Phys. Lett. 61B, 303 (1976).
[17]Our result is consistent with the value $\sigma(\gamma)=252\pm18$ mb reported in Ref. 7.
[18]G. J. Donaldson *et al.*, Phys. Rev. Lett. 40, 684 (1978).
[19]F. T. Dao and J. Whitmore, Phys. Lett. 46B, 252 (1973).
[20]D. Horn and A. Schwimmer, Nucl. Phys. B52, 627 (1973); D. Drijard and S. Pokorski, Phys. Lett. 43B, 509 (1973); P. Grassberger and H. I. Miettinen, Nucl. Phys. B82, 26 (1974); B89, 109 (1975); A. Arneodo and J. Kubar-Andre, *ibid.* B77, 309 (1974); Lett. Nuovo Cimento 12, 1 (1975).
[21]Only pion production is treated by the models. In our data the identity of the charged particles is not determined, hence comparison of models with data is meaningful to the extent that pions are the most abundant species of particles produced in 300-GeV/c pp collisions. [See M. Antinucci *et al.*, Lett. Nuovo Cimento 6, 121 (1973).]
[22]G. H. Thomas, Phys. Rev. D 8, 3042 (1973).
[23]F. T. Dao, in *Particles and Fields—1974*, Proceedings of the 1974 Williamsburg Meeting of the Division of Particles and Fields of the American Physical Society, edited by Carl E. Carlson (AIP, New York, 1975), p. 199.
[24]S. Barish *et al.*, Phys. Rev. Lett. 31, 1080 (1973); F. T. Dao *et al.*, Phys. Lett. 45B, 399 (1973).
[25]A. W. Chao and C. Quigg, Phys. Rev. D 9, 2016 (1974); A. Arneodo and G. Plaut, Nucl. Phys. B107, 262 (1976).